

## About this Article

This material was included with the downloadable supplemental content accompanying the *ARRL Antenna Book*.

You may print a copy of this material for personal use. Any other use of the information requires permission from the ARRL.

## Copyright/Reprint Notice

In general, all ARRL content is copyrighted. ARRL articles, pages, or documents – printed and online – are not in the public domain. Therefore, they may not be freely distributed or copied. Additionally, no part of this document may be copied, sold to third parties, or otherwise commercially exploited without the explicit prior written consent of the ARRL. You cannot post this document to a website or otherwise distribute it to other through any electronic medium.

For permission to quote or reprint material from ARRL, send a request including the issue date, a description of the material requested, and a description of where you intend to use the reprinted material to the ARRL Editorial and Production staff at: **[permission@arrl.org](mailto:permission@arrl.org)**.

# *The Multiband Extended Double Zepp and Derivative Designs*

---

*W7SX's search for simple multiband antennas with bidirectional patterns continues. Here are several new examples to cover 14, 18, 21, 24, 28 and 50 MHz, 7, 10, 14 and 21 MHz, 21 and 50 MHz and a W8JK derivative for 14 through 50 MHz. Grab your rope and wire cutters!*

---

By Robert J. Zavrel Jr, W7SX

The great reader response to "Multiple-Octave Bidirectional Wire Antennas" in the July/August 1998, issue of *QEX* prompted me to look more closely at the  $\lambda/4$  stub technique. This stub provides both linear end loading on lower frequencies and an effective trap at the frequency where the stub is  $\lambda/4$ . The original antennas were built to provide multiband bidirectional operation from a single design. Two configurations were constructed: one for 80/40/20-meter operation and one for 40/30/20/10-meter operation. Further analysis has yielded some interesting interre-

relationships in this design. This paper reports these findings.

Fig 1 shows the fundamental design of this antenna. The highest frequency ( $f_h$ ) of operation (for a bidirectional pattern) is defined where  $L_i$  is chosen as an equivalent length for a double extended Zepp. The length of the end-shortened stub ( $L_s$ ) is  $\lambda/4$  at this same frequency. Therefore, the total antenna length is  $1.75\lambda$  (free space) at  $f_h$ . At  $f_h$ , there is a current maximum at the very ends of the antenna. However, the equal currents flowing in either side of the stub are out of phase, thus the radiation pattern contribution from these currents cancel. These current maximums therefore do not contribute to the pattern of the array at this frequency, where  $L_s = \lambda/4$ . Consequently, the only portion of the an-

tenna that contributes to the pattern is the single-wire section, which corresponds to an extended double Zepp at  $f_h$ . In effect, a  $\lambda/4$  shorted stub located at the end of an antenna element will act like a trap, with the effective trap location being the open end of the stub. This is true for any element configuration, and can be used in a variety of schemes. To this date, I have not found a configuration that will permit a multiband stub trap, or use of the stub anywhere but the end of an antenna element.

Above and below  $f_h$ , the currents do not cancel, and currents in the stub contribute to the radiation pattern of the antenna overall. This results in the "four-leaf" pattern, similar to that of simple long wires. As frequency is reduced further, the four-leaf lobes

---

745 Royal Crown Ln  
Colorado Springs, CO 80906  
[w7sx@aol.com](mailto:w7sx@aol.com)

gradually decrease and bidirectional lobes gradually increase, until an extended double Zepp pattern returns. I define this as  $f_i$ , or the intermediate bidirectional frequency. The ratio of  $f_h/f_i$  for wire antennas in the HF range is about 1.61. Therefore, this antenna will exhibit the equivalent extended double Zepp gain and bidirectional pattern at two frequencies whose ratio is about 1.61.

As the frequency of operation is reduced below  $f_i$ , a bidirectional pattern is maintained, but with lesser broadside gain. This is exactly as we expect from a “normal” extended double Zepp. This gain gradually decreases to that of a simple dipole. I define this frequency as  $f_d$ . The ratio  $f_h/f_d$  is about 3.57.

Figs 2 and 3 plot gain versus  $f_h$ ,  $f_i$ , and  $f_d$  for the Antennas 1 and 2. A 0 dBd ( $\lambda/2$  dipole reference broadside gain) line is shown for convenience of comparison. All plots are free-space diagrams; the wire elements are #12 copper wire. Stub wire spacing is 0.1 feet, similar to the standard 450- $\Omega$  ladder-line spacing that was used in the original arrays. Two graphs show the relationship between broadside gain and frequency for the simple, in-line antenna elements.

### Modeling Notes

I used EZNEC Version 2.0 for all these configurations. I noticed that the antenna patterns and feed-point impedances changed radically when changing the number of segments used in the models. For more-accurate results, Roy Lewallen, W7EL, suggests using *many* more segments than would normally be used in arrays of these dimensions.<sup>1</sup> See the sidebar “Modeling Closely Spaced Wires.” The current-canceling characteristics of the stub seem to be the main problem. In addition, the number and alignment of segments used in the  $\lambda/4$  stub wire should be parallel with the segments in the opposite wire—the respective portions of  $L_t$  in Fig 1. (That is, the numbers of segments in the upper and lower wires of the stub should be equal, and the segment-end points should align vertically. See Fig 1 inset—Ed.)

I used five wires to model these arrays in EZNEC. Wire 1 corresponds to  $L_t$  in Fig 1. Wires 2 and 3 represent the 0.1-foot shorting wires at the antenna’s ends (use one segment each for these short wires). Wires 4 and 5 represent the parallel stub wires. The number of segments used is listed for both

$L_t$  and  $L_s$  in the two sample antennas. The points on Figs 2 and 3 are actual broadside gain numbers taken from the numerous simulation runs.

### Some Practical Single-Wire Designs

A quick analysis of the dual-peak broadside-gain characteristics opens some very interesting possibilities for amateur multiband applications.

Three separate wire-antenna dimensions are presented for multiband use:

Antenna 1: 14/18/21/25/28/50 MHz

$L_t = 34.4$  ft

$L_s = 4.9$  ft

$f_h = 50$  MHz

$f_i = 31$  MHz

$f_d = 14$  MHz

85 segments used for  $L_t$  (Fig 1)

12 segments used for each  $L_s$  (Fig 1)

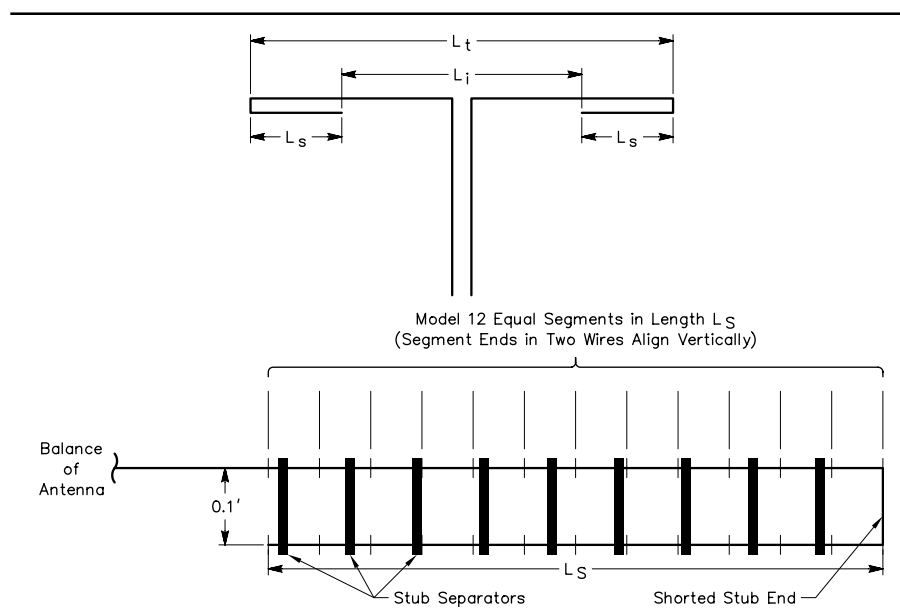


Fig 1—Antennas 1 and 2 are built from this plan.  $L_s$  is the length of the end-loading stubs, which act as shorted  $\lambda/4$  transmission-line stubs at  $f_h$ . At  $f_h$ ,  $L_i$  is  $1.25 \lambda$ ;  $L_s$  is  $\lambda/4$ ;  $L_t$  is  $1.75 \lambda$ . Inset shows details of stub model and construction. Dimensions for each antenna are given in the text. Drawing not to scale.

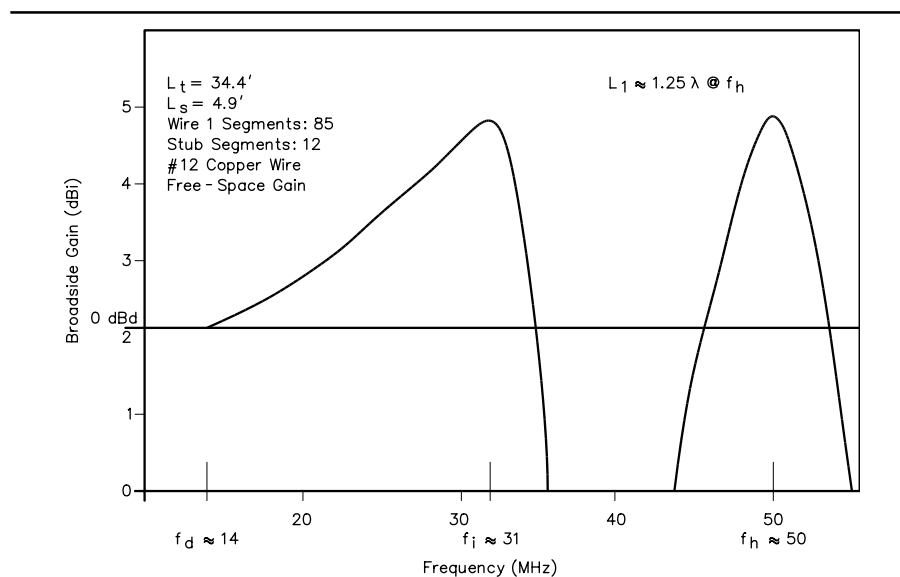


Fig 2—Antenna 1 broadside gain (dBi) versus frequency.

<sup>1</sup>Notes appear on page 39.

This antenna can provide significant bidirectional gain over six amateur bands, with the gain peaks appearing at six and just above 10 meters. (See Fig 4.) The actual ratio of 50.1/28.1 MHz is about 1.78, a bit more than the 1.61 for this antenna. However, the 10-meter gain is only about 0.5 dB below that of an extended double Zepp, and gain on all amateur frequencies above 14 and below 51 MHz is better than a dipole. This might be an attractive array for the sunspot-cycle peak, with optimum response on six and 10 meters.

#### Antenna 2: 7/10/14/21 MHz

$$L_t = 74.0 \text{ ft}$$

$$L_s = 12.46 \text{ ft}$$

$$f_h = 21 \text{ MHz}$$

$$f_i = 14 \text{ MHz}$$

$$f_d = 7 \text{ MHz}$$

85 segments used for  $L_t$  (Fig 1)

14 segments used for each  $L_s$  (Fig 1)

This interesting antenna provides an extended-double-Zepp response at both the 14 and 21 MHz bands, as well as some broadside gain at 10.1 and 7 MHz. (See Fig 5.) At 18.1 MHz, the antenna pattern resembles a four-leaf long wire, the broadside gain being just about 0 dBi.

When the desired frequency ratio for the two gain peaks is less than 1.61, as is the case for 21.1 and 14.1 MHz,  $L_i$  can be decreased. However, I noticed that about 5 dBi gain could be maintained by a slight lengthening of  $L_s$ . By experimenting with exact lengths, the desired dual-peak frequency ratio of 1.5 can be obtained, with  $L_i$  about  $1 \lambda$  rather than  $1.25 \lambda$ . This antenna has a response equivalent to an extended double Zepp at both 15 and 20 meters! It also has gain at 10.1 MHz and has a simple dipole response on 40 meters.

#### Antenna 3: 21/50 MHz

$$L_t = 18.1 \text{ ft}$$

$$L_s = 5.1 \text{ ft}$$

$$f_h = 50 \text{ MHz}$$

$$f_d = 21 \text{ MHz}$$

85 segments used for  $L_t$

24 segments used for  $L_s$

Here,  $L_i$  is chosen to be near  $\lambda/2$  rather than  $1.25 \lambda$  at  $f_h$  and  $L_s$  is chosen to be the predefined  $\lambda/4$  stub. In this case, the bidirectional gain at both  $f_h$  and  $f_d$  will approximate a simple dipole. However, the feed-point impedance at both  $f_h$  and  $f_d$  will also approximate a simple dipole (in practice between about 50 and 100  $\Omega$ ). For these dimensions, the ratio will be about 2.38, which is exactly the correct ratio for 50 and 21 MHz!

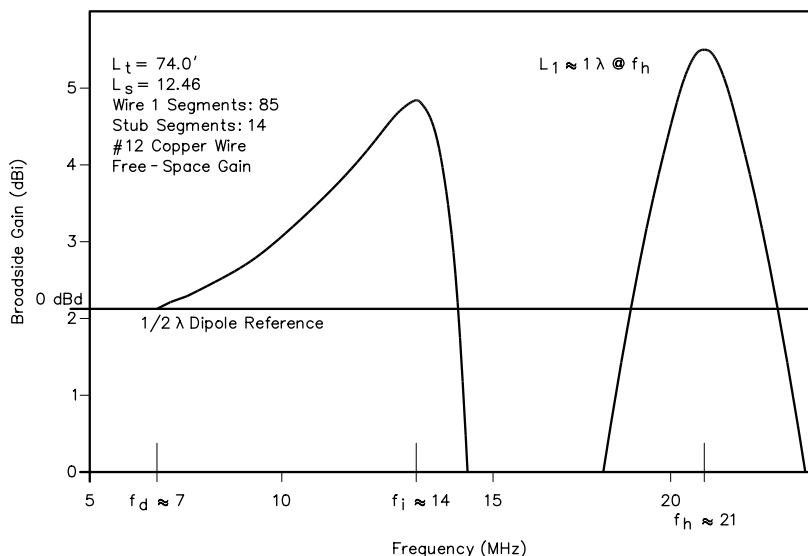


Fig 3—Antenna 2 broadside gain (dBi) versus frequency.

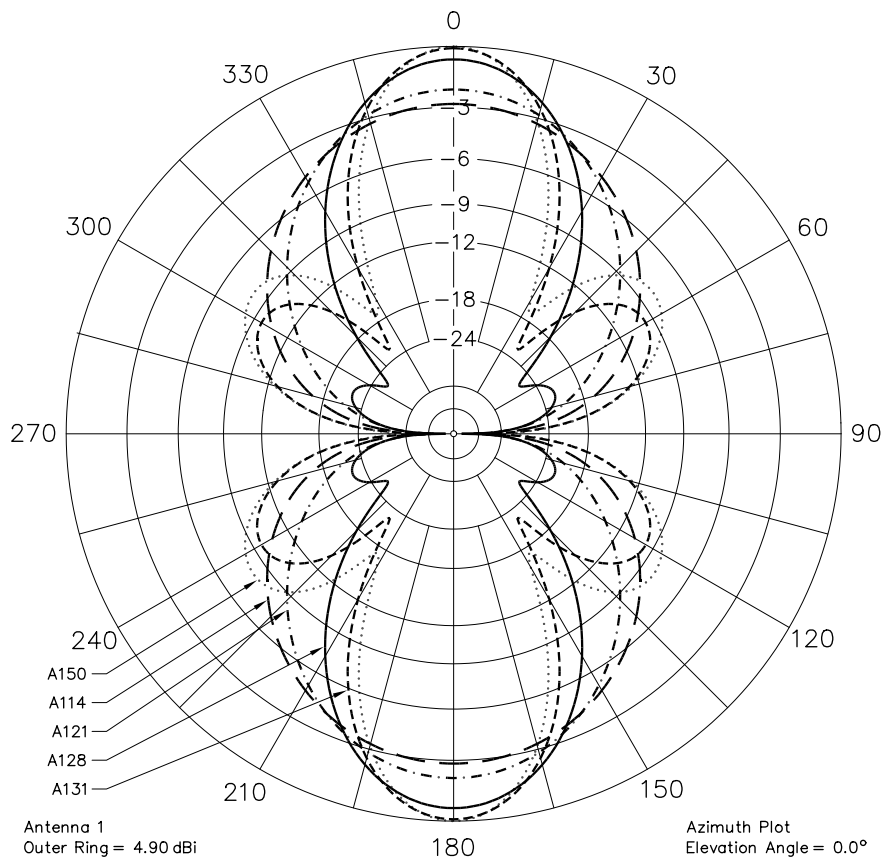


Fig 4—Antenna 1 free-space azimuthal radiation-pattern plots at 0° elevation for several frequencies. A114 indicates Antenna 1 at 14 MHz; A121 indicates Antenna 1 at 21 MHz, etc.  $14.15 \text{ MHz} = f_i$ ;  $f_d < 21 \text{ MHz} < f_i$ ;  $28.1 \text{ MHz} < f_i$ ;  $31 \text{ MHz} = f_i$ ;  $50 \text{ MHz} = f_h$ .

The exact ratio was achieved by experimenting (as with Antenna 2) with small derivations of  $L_t$  and  $L_s$ . The best compromise was found to be a feed-point impedance of about 100  $\Omega$  at 50 MHz. This impedance was “lowered” by adding two parasitic elements and

thus forming a three-element, 6-meter Yagi. (See Fig 6.) A 15-meter reflector could also be added, but the SWR will increase to about 2:1. Left as a dipole, it is near 1:1 on 15 meters. With the actual feed-point impedance near 50  $\Omega$  on both 6 and 15 meters, in effect, a

“free” 15-meter rotatable dipole can be built into a “normal” 6-meter Yagi. The driven element is simply fed through a 1:1 balun and 50- $\Omega$  feedline.

This antenna was modeled using #12 copper wire, so an aluminum-tube Yagi’s dimensions and taper schedule would have to be optimized. Fig 7 shows radiation patterns for 21 and 50 MHz.

### W8JK and Yagi Configurations

We can make a very effective two-element array using two extended double Zepps—like Antenna 1—configured as a W8JK array. (See Fig 8.) The bidirectional gain is roughly equivalent to a three-element Yagi in

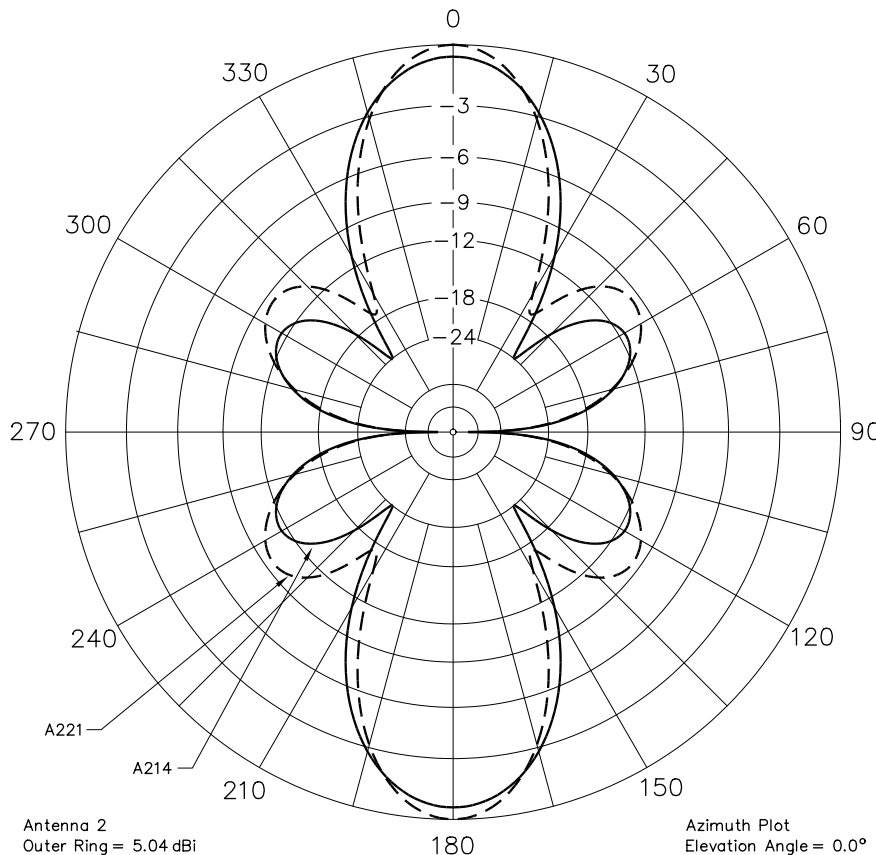


Fig 5—Antenna 2 free-space azimuthal radiation-pattern plots at 0° elevation for two frequencies. A214 indicates Antenna 2 at 14 MHz ( $f_h$ ); A221 indicates Antenna 2 at 21 MHz ( $f_h$ ).

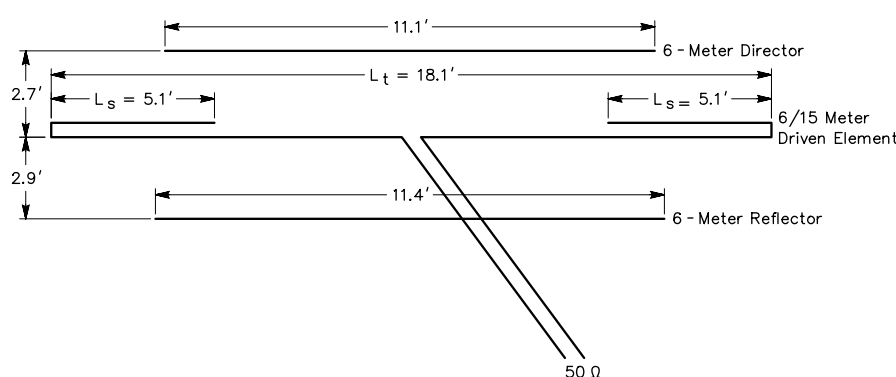


Fig 6—Antenna 3 is built from this schematic, a bottom view. It acts as a three-element beam at 6 meters, but functions as a simple dipole at 15 meters.

### Modeling Closely Spaced Wires with NEC-2

Closely spaced wires carrying very different currents are a bit tricky to model with EZNEC and other NEC-2 based programs. One important thing is to make the segment junctions on the parallel wires align with each other as closely as possible. As sent, the model reports a source impedance of 1263  $-j2335\Omega$ . I changed wire 1 to 43 segments to more closely match its segment junctions with those of the loading wires. The result was 254  $-j1372\Omega$ . Actually, 42 segments is closer, but an odd number is required so that the source can be at the antenna center (unless a split source is used), so I also tried 41 for wire 1. The result was then 275  $-j1415\Omega$ , not a large difference. Then I doubled the number of segments, keeping them aligned on the parallel wires. With 85 segments for wire 1 and 12 for the loading wires, it reported 325  $-j1481\Omega$ . Approximately doubling again to 169 and 24 segments gave 366  $-j1535\Omega$ . I'd say from this that wire 1 should have at least 85 segments for good results. More than that will improve accuracy some, but not a great deal. Now here's the interesting part: With wire 1 held at 169 segments, I changed the number of segments on the loading wires from 24 to 36, greatly disturbing the alignment of the segment junctions. The impedance changed to 366  $-j1536\Omega$ —almost no change at all from the value with 24 segments. This shows that it's much more important to line up the segment junctions when the segment lengths are comparable to the wire spacing than when the segments are shorter.—Roy Lewallen, W7EL

both directions at  $f_h$  and  $f_i$ . (See Fig 9.) Therefore, a rotatable two-element W8JK using Antenna 1's element dimensions (modified for tapered tubing elements) could provide quite impressive gain over six amateur bands. The array modeling here used six-foot spacing. However, this spacing drops the feed-point impedance to a low value at 14 and 18 MHz. This problem can be solved by placing a relay at the element feed points. By using a 61-pF capacitor inserted in line at the element's center, a reflector element is created at 14 MHz, and the feed-point impedance is changed to a more acceptable value. There is a common misconception that the driven element in a Yagi array must be a resonant dipole. In fact, the only critical electrical lengths are those of the parasitic elements and their spacing. Even the parasitic-element lengths can be tuned by appropriate reactive loads, as the example above shows.

Here is an interesting possibility: Because the two elements are identical, either element may be switched into the reflector mode. Thus, the main pattern lobe may be easily and instantaneously reversed ( $180^\circ$ ) at 14 MHz by placing a relay and 61-pF capacitor at the center of each element. This is very useful because one can instantly check whether a signal is arriving via short or long path without physically rotating the Yagi. Therefore, it is quite practical to configure the two-element antenna to provide a switchable pattern ( $0^\circ$  and  $180^\circ$  azimuth for 20 meters) and a W8JK bidirectional pattern for bands from 14 through 50 MHz. Of course, with added switching complexity, a unidirectional pattern could be configured at 18 and perhaps 21 MHz. This feature would be very useful for working gray-line DX, nets and contests.

Note that getting the exact required reactive values from NEC and NEC-based modeling programs is difficult. Some tweaking will be required to optimize front-to-back ratios and/or maximize forward gain.

The combinations seem endless. The essential point is that this antenna is the same size as, and has comparable hardware to, a standard two-element, 20-meter Yagi, yet it can show excellent gain performance on all bands from 20 up to 6 meters. Two Antenna-2 elements could be fashioned into a W8JK as well, to provide similar gain characteristics on 40, 30, 20 and 15 meters. It is important that for short spacings in the W8JK configuration, the feed-point impedance can become difficult to

## What about Ground Effects?

The antennas in this article are modeled in free space. That's fine for general comparisons of the major-lobe signal strength among several antennas. It's a good idea, however, to look at the big picture as well. To do that, we need to put the antenna over real earth and view the elevation plot as well as the azimuth plot. As an example, I've taken W7SX's Antenna 1, placed it 35 feet above real ground (0.005 S/m,  $\epsilon = 13$ ) and screen captured three-dimensional plots for EZNEC2 high-accuracy ground analyses. The antenna placed  $\lambda/2$  above real ground exhibits take-off angles greater than  $0^\circ$ , and the nulls are largely filled by ground reflections (Fig A). As the height increases—with respect to  $\lambda$ —the antenna may show lesser lobes above the main lobe. At some frequencies and heights, there is significant vertical radiation (Fig B). Similar effects remain, even when the antenna is 125 feet high.—Bob Schetgen, KU7G

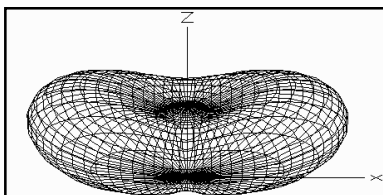


**Fig A—Antenna 1 at 14 MHz, modeled 35 feet ( $\lambda/2$ ) above real ground. The takeoff angle is about  $25^\circ$ . We can consider this the best-case ground effect for this antenna.**

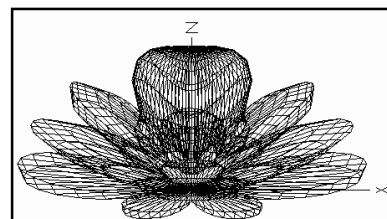


**Fig B—Antenna 1 at 50 MHz, modeled 35 feet ( $1.77 \lambda$ ) above real ground. The takeoff angle is about  $10^\circ$ . We can consider this the worst-case ground effect for this antenna.**

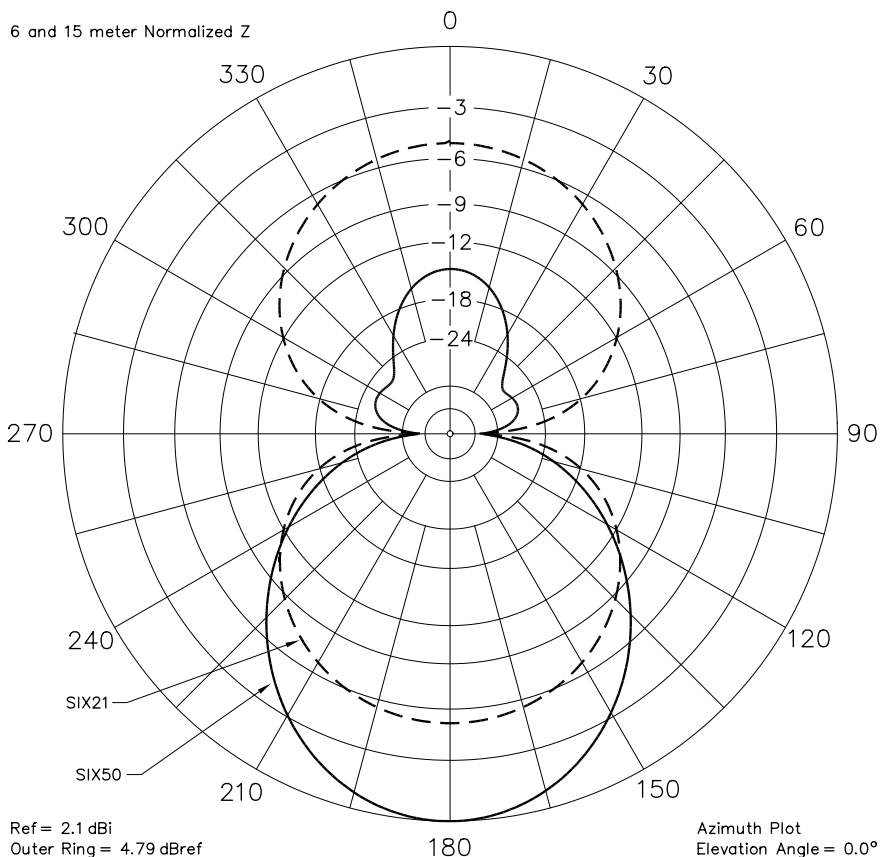


**Fig 7—Antenna 3 free-space azimuthal radiation-pattern plots at  $0^\circ$  elevation for two frequencies. SIX21 indicates Antenna 3 at 28.1 MHz; SIX50 indicates Antenna 3 at 50 MHz.**

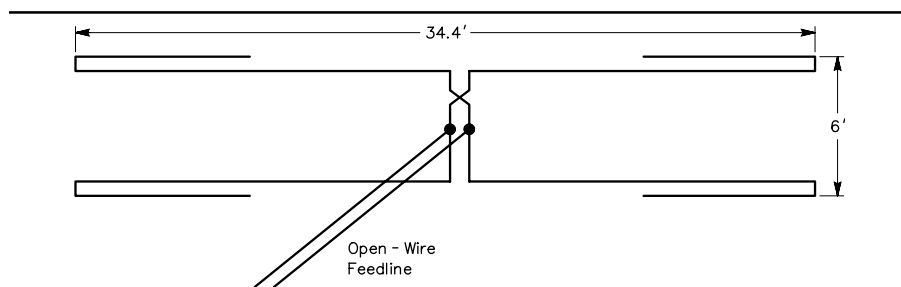


**Fig 8**—This schematic shows a W8JK-style array (I call it W8JK-EDZ) made from two elements, each with dimensions as shown for Antenna 1; it's a bottom view. Both elements lie in a horizontal plane.

match as operating frequency approaches  $f_d$ . This is the motivation for switching to a parasitic array at and near  $f_d$ , not to mention greater gain at these lower frequencies!

Except for Antenna 3, I've assumed that these antennas have open-line feeds, with a tuner placed in some convenient location. I used 450- $\Omega$  ladder line in the original arrays I built, and tuned to the operating frequency in the shack. However, more intensive modeling with a Smith Chart software tool—such as *MicroSmith*—might reveal some clever multiband scheme that matches to 50  $\Omega$ .

## Conclusion

Similar gain numbers are possible for other frequencies by appropriately scaling lengths and spacing. By simply replacing  $\lambda/2$ -dipole wires with this element, many of the familiar array configurations shown in the *ARRL Antenna Book* and other texts take on new dimensions of gain versus frequency. Yet, this basic antenna element is lightweight, inexpensive and easy to build. In the battle to squeeze a few more decibels of gain out of a given space, I hope this technique will be considered as an interesting decibel/dollar option.

## Note

<sup>1</sup>"Convergence testing consists of increasing the number of segments per unit of length equally throughout the antenna structure and observing changes in the output data for parameters significant to the modeling exercise." This definition is taken from "NEC-4.1: Limitations of Importance to Hams," by L. B. Cebik, W4RNL (*QEX*, May/June 1998, pp 3-16). When increasing the number of segments significantly changes some result, say feed impedance, it indicates that the previous results are in error because there were too few segments. When the results change little with added segments, they are said to converge and are considered accurate. Readers can learn more about modeling limitations from Mr. Cebik's article and "Wire Modeling Limitations of NEC and MININEC for Windows" by John Rockway and James Logan, N6BRF (*QEX*, May/June 1998, pp 17-21).

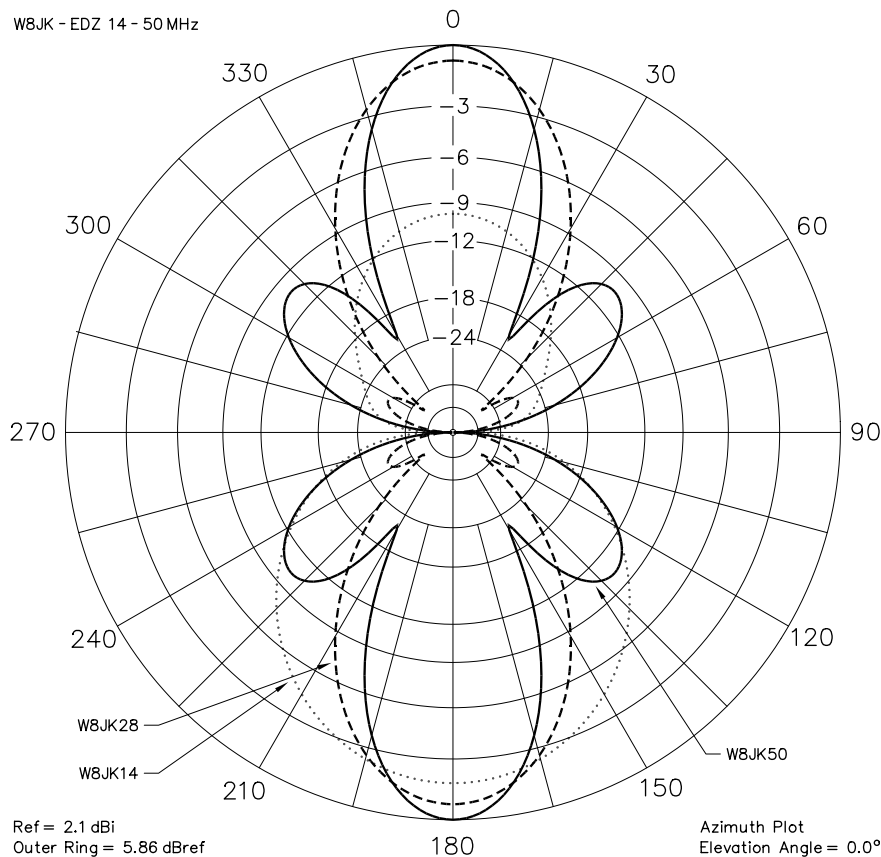


**Fig 9**—W8JK-EDZ free-space azimuthal radiation-pattern plots at 0° elevation for two frequencies. W8JK28 indicates W8JK-EDZ at 28 MHz ( $28.1 \text{ MHz} = f_1$ ); W8JK50 indicates W8JK-EDZ at 50 MHz ( $50 \text{ MHz} = f_2$ ). W8JK14 indicates a W8JK-EDZ operated as a 14.1-MHz, two-element Yagi. The Yagi is just as shown in Fig 8, except only one element is fed and the other loaded with a series connected 61 pF capacitor at its center.